Ultramicroscopy 134 (2013) 18–22

Contents lists available at ScienceDirect

Ultramicroscopy

journal homepage: www.elsevier.com/locate/ultramic

The interaction of a nanoscale coherent helium-ion probe with a crystal

A.J. D'Alfonso, B.D. Forbes, L.J. Allen *

School of Physics, University of Melbourne, Parkville, Victoria 3010, Australia

ARTICLE INFO

Available online 3 July 2013

Keywords:
Helium ion microscopy
Atomic resolution imaging
Ion scattering theory

ABSTRACT

Thickness fringing was recently observed in helium ion microscopy (HIM) when imaging magnesium oxide cubes using a 40 keV convergent probe in scanning transmission mode. Thickness fringing is also observed in electron microscopy and is due to quantum mechanical, coherent, multiple elastic scattering attenuated by inelastic phonon excitation (thermal scattering). A quantum mechanical model for elastic scattering and phonon excitation correctly models the thickness fringes formed by the helium ions. However, unlike the electron case, the signal in the diffraction plane is due mainly to the channeling of ions which have first undergone inelastic thermal scattering in the first few atomic layers so that the origin of the thickness fringes is not due to coherent interference effects. This quantum mechanical model affords insight into the interaction of a nanoscale, focused coherent ion probe with the specimen and allows us to elucidate precisely what is needed to achieve atomic resolution HIM.

1. Introduction

Helium ion microscopy (HIM) is an analytic technique that has been used for imaging at the nanoscale and a resolution of 0.24 nm has been achieved [1]. Imaging in HIM has typically been performed using secondary electrons which exit the entrance surface of the specimen [2]. The feasibility of operating in transmission mode, scanning transmission helium ion microscopy (STHIM), has only recently been explored in any detail [3]. Nanometer scale resolution imaging was demonstrated using a convergent 40 keV He_4^+ beam to image MgO particles as a function of thickness. An apparently diffraction-related phenomenon was observed, namely thickness fringing, as shown in Fig. 1(a). The inset shows thickness fringes obtained from a ⟨110⟩ oriented MgO nanocube [3]. The experimental points are from two scans taken at right angles to the fringes. Thickness fringing is also observed in electron diffraction and is due to coherent multiple elastic scattering of the electrons, attenuated by thermal diffuse scattering (TDS) due to phonon excitation [4].

In this paper we use a quantum mechanical model to simulate HIM. Using this model we see that the thickness fringes become apparent *after* substantial inelastic scattering because TDS has occurred in the first few atomic layers in the crystal (perhaps multiple times). Therefore the origin of the thickness fringes is not due to coherent interference effects, as is the case in electron microscopy. Our model provides an understanding of what is needed to achieve atomic resolution HIM. Forbes et al. [5] recently developed a model for the elastic scattering and the inelastic scattering due to phonon excitation by fast electrons incident on a crystal—referred to here as the QEP (quantum excitation of phonons) model. The quantum mechanical underpinnings of this approach are in contrast to the frozen phonon model [6,7]. The model has the advantage that the contribution to the signal in the diffraction plane can be separated into the component which is due to elastic scattering and that which is due to TDS. It has recently been successfully applied in the context of scanning transmission electron microscopy (STEM) imaging to explain apparent anomalies in the oxygen signal in strontium titanate using both electron energy-loss spectroscopy and energy-dispersive X-ray analysis [8]. In a similar way, here we use the QEP model to provide insights into the interaction of a focused, coherent, nanoscale helium-ion probe with a crystal. Classical (Monte Carlo) models [2,9] correctly predict channeling patterns from a single crystal, as established several decades ago—see for example Refs. [10,11]. However, here we use the quantum mechanical QEP model for the physical insight it provides concerning the interaction of the nanoscale probe with the specimen and the clear understanding it then gives regarding what is needed to achieve atomic resolution imaging in HIM.

2. Theory

The QEP model starts from the many-body Schrödinger equation for the incident particle plus all the nuclei and electrons in the target. It is applicable not only to electrons but also to any charged

* Corresponding author. Tel.: +61 3 8344 7402; fax: +61 3 9347 4783.
E-mail address: lja@unimelb.edu.au (L.J. Allen).

0304-3991/$ - see front matter © 2013 Elsevier B.V. All rights reserved.
http://dx.doi.org/10.1016/j.ultramic.2013.06.019

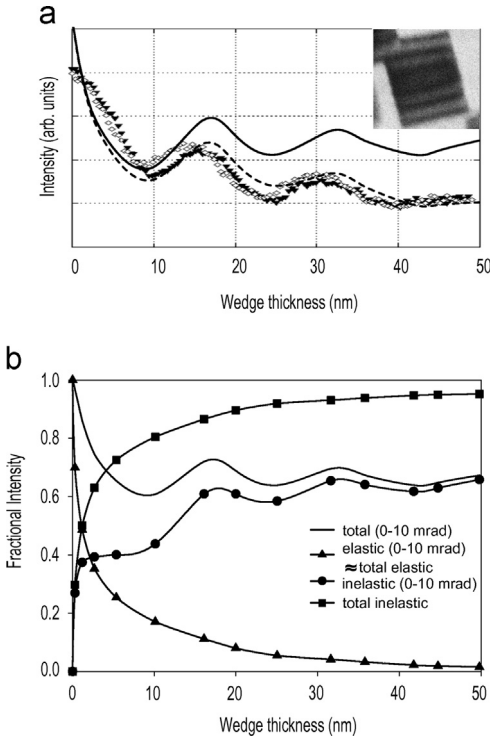

Fig. 1. (a) Inset: Thickness fringes formed by a convergent 40 keV He_4^+ ion probe incident on ⟨110⟩ MgO using a detector with an acceptance semi-angle of 10 mrad. Experimental points are line scans normal to the fringes (open and closed markers indicate data from either side of the central maximum). Data from Ref. [3]. The solid line is the fringing predicted by the QEP model and the dashed line further takes into account absorption due to ion–electron interactions. (b) The QEP model calculation in (a) decomposed into the contribution from elastically scattered ions and those that have been inelastically scattered (thermally). Also indicated are the total elastic and total inelastic contributions in the diffraction plane (i.e. including scattering outside the 10 mrad detector).

incident particle for which the assumptions and approximations made hold. The many body wave function for the incident particle plus target is written in the form

$$\Psi(\mathbf{r},\boldsymbol{\tau}_n,\boldsymbol{\tau}_e)=a(\boldsymbol{\tau}_n)b(\boldsymbol{\tau}_e)\phi(\mathbf{r},\boldsymbol{\tau}_n), \tag{1}$$

here $\mathbf{r}$ refers to the co-ordinate of the incident particle (in this context an ion), $\boldsymbol{\tau}_n$ is the set of nuclear co-ordinates and $\boldsymbol{\tau}_e$ designates the set of all the co-ordinates of the electrons in the target. The term $a(\boldsymbol{\tau}_n)b(\boldsymbol{\tau}_e)$ represents a crystal eigenstate and it has been assumed that the electron and nuclear subsystems can be decoupled for the purposes of considering phonon excitation, which is an interaction of the incident ion with the nuclear subsystem. The quantity $\phi(\mathbf{r},\boldsymbol{\tau}_n)$ is associated with the incident ion. The key assumption we make is that $a(\boldsymbol{\tau}_n)$ might be chosen such that $\phi(\mathbf{r},\boldsymbol{\tau}_n)$ satisfies

$$\nabla_{\boldsymbol{\tau}_n}\phi(\mathbf{r},\boldsymbol{\tau}_n)\approx\mathbf{0}, \tag{2}$$

allowing us to neglect such derivatives of $\phi(\mathbf{r},\boldsymbol{\tau}_n)$. It is shown in Ref. [5] that the ground state of the nuclear subsystem is a good choice for $a(\boldsymbol{\tau}_n)$. The assumption in Eq. (2) is akin to the Born–Oppenheimer approximation, used in molecular physics, for the function $\phi(\mathbf{r},\boldsymbol{\tau})$ associated with the ion. Physically this means that $\phi(\mathbf{r},\boldsymbol{\tau}_n)$ is insensitive to *variations* in the co-ordinates of the crystal nuclei. This is consistent with the disparity in energy between the incoming ion (tens to thousands of keV) and the energy associated with exciting phonons in the nuclear subsystem (meV).

The probability distribution of the ion in the plane defined by the co-ordinate $\mathbf{r}_\perp$ at a depth z in the crystal [or at any plane beyond the crystal having propagated the $\phi(\mathbf{r},\boldsymbol{\tau})$ at the exit surface] is obtained by a quantum-mechanical average over the nuclear coordinates, using Eq. (1), as

$$\begin{aligned} I(\mathbf{r})\equiv I(\mathbf{r}_\perp,z) &= \int |\Psi(\mathbf{r}_\perp,z,\boldsymbol{\tau}_n,\boldsymbol{\tau}_e)|^2\, d\boldsymbol{\tau} \\ &= \int |\phi(\mathbf{r}_\perp,z,\boldsymbol{\tau}_n)|^2|a(\boldsymbol{\tau}_n)|^2\, d\boldsymbol{\tau}_n \int |b(\boldsymbol{\tau}_e)|^2\, d\boldsymbol{\tau}_e \\ &= \int |\phi(\mathbf{r}_\perp,z,\boldsymbol{\tau}_n)|^2|a(\boldsymbol{\tau}_n)|^2\, d\boldsymbol{\tau}_n, \end{aligned} \tag{3}$$

where the integration over the electronic degrees of freedom is assumed to be normalized to unity and $|a(\boldsymbol{\tau}_n)|^2$ is acting as a probability distribution. The function $\phi(\mathbf{r}_\perp,z,\boldsymbol{\tau}_n)$ satisfies a Schrödinger-like equation with an interaction potential $V(\mathbf{r},\boldsymbol{\tau}_n)$ [5] that we solve using the well-known multislice method [12]. The probability distribution $|a(\boldsymbol{\tau}_n)|^2$ can be calculated assuming that the nuclear subsystem is modeled as a set of independent harmonic oscillators (a so-called Einstein model), as discussed in Ref. [5], with input being the Debye–Waller factors (related to the root-mean-square thermal displacements) of the various atoms in the specimen. The probability distribution in reciprocal space (i.e. in the diffraction plane) is obtained by replacing $\phi(\mathbf{r}_\perp,z,\boldsymbol{\tau}_n)$ in Eq. (3) by its Fourier transform. The interaction potential $V(\mathbf{r},\boldsymbol{\tau}_n)$, for a given configuration $\boldsymbol{\tau}_n$, is written as

$$V(\mathbf{r},\boldsymbol{\tau}_n)=\sum_{\mathbf{g}}V_{\mathbf{g}}(\boldsymbol{\tau}_n)\exp(2\pi i\mathbf{g}\cdot\mathbf{r}), \tag{4}$$

where the Fourier coefficients $V_{\mathbf{g}}$ are given by

$$V_{\mathbf{g}}=\frac{1}{V_c}\sum_j\exp(-2\pi i\mathbf{g}\cdot\boldsymbol{\tau}_{nj})f_j(g), \tag{5}$$

here $\mathbf{g}$ are reciprocal lattice vectors, V_c is the volume of the unit cell, $\boldsymbol{\tau}_{nj}$ explicitly refers to the position of atom j in the unit cell for configuration n and $f_j(g)$ is the atomic scattering factor for atom j, given by

$$f_j(s)=\frac{8\pi^2me}{h^2}\int_0^\infty r^2V_j(r)\frac{\sin(4\pi sr)}{4\pi sr}\,dr, \tag{6}$$

where conventionally $s\equiv g/2$. The mass of the ion is m and e is the magnitude of the charge of an electron. The scattering potential $V_j(r)$ of the jth atom is assumed to be spherically symmetric and is repulsive. We use the parameterization for the scattering potential V_j given in Ref. [13]:

$$V_j(r)=-\frac{1}{4\pi\epsilon_0}\frac{QQ'}{r}\sum_{i=1}^{4}\alpha_i\exp\left(-\frac{\beta_i r}{a}\right), \tag{7}$$

where ϵ_0 is the permittivity of free space, $Q=Ze$ and $Q'=Z'e$ are the net charges of the projectile and the charge of the nucleus of the target atom labeled by j and a is the screening radius. The parameters in Eq. (7) are as follows:

$$\begin{aligned} &\alpha_i=\{0.1818,0.5099,0.2802,0.02817\} \\ &\beta_i=\{3.2000,0.9423,0.4029,0.2106\} \\ &a=\frac{0.8853a_B}{Z^{0.23}+(Z')^{0.23}}, \end{aligned} \tag{8}$$

with a_B being the Bohr radius. Here we are considering the scattering of He_4^+ from MgO. Therefore $Z=1$ and Z' is either 8 (O) or 12 (Mg). The potential $V(\mathbf{r},\boldsymbol{\tau}_n)$, as given by Eq. (4), is shown in Fig. 2(a) projected over a unit cell for He_4^+ ions incident along the [110] zone axis in MgO for one possible configuration of the atoms $\boldsymbol{\tau}_n$.

3. Simulations

Using an ensemble of potentials generated assuming an Einstein model [5] and taking the Debye–Waller factors from Ref. [14], we have simulated the experimental thickness fringes in Fig. 1(a)